Biochimica et Biophysica Acta 1808 (2011) 2045–2050

Contents lists available at ScienceDirect

Biochimica et Biophysica Acta

journal homepage: www.elsevier.com/locate/bbamem

The A391E mutation enhances FGFR3 activation in the absence of ligand

Fenghao Chen [a], Catherine Degnin [b], Melanie Laederich [b], William A. Horton [b], Kalina Hristova [a,*]

[a] Department of Materials Science and Engineering, Johns Hopkins University, Baltimore, MD 21218, USA
[b] Department of Molecular & Medical Genetics, Oregon Health & Science University, Research Center, Shriners Hospital for Children, Portland, OR 97239, USA

ARTICLE INFO

Article history:
Received 31 January 2011
Received in revised form 11 April 2011
Accepted 12 April 2011
Available online 22 April 2011

Keywords:
Membrane proteins
Cell signaling

ABSTRACT

The A391E mutation in the transmembrane domain of fibroblast growth factor receptor 3 leads to aberrant development of the cranium. It has been hypothesized that the mutant glutamic acid stabilizes the dimeric receptor due to hydrogen bonding and enhances its ligand-independent activation. We previously tested this hypothesis in lipid bilayers and showed that the mutation stabilizes the isolated transmembrane domain dimer by −1.3° kcal/mol. Here we further test the hypothesis, by investigating the effect of the A391E mutation on the activation of full-length fibroblast growth factor receptor 3 in Human Embryonic Kidney 293T cells in the absence of ligand. We find that the mutation enhances the ligand-independent activation propensity of the receptor by −1.7° kcal/mol. This value is consistent with the observed strength of hydrogen bonds in membranes, and supports the above hypothesis.

1. Introduction

The fibroblast growth factor receptors (FGFR1, 2, 3, and 4) play a critical role in the development of the skeletal system [1–3]. These receptor tyrosine kinases (RTKs) have extracellular domains consisting of glycosylated Ig-like domains, single transmembrane (TM) domains, and characteristic split tyrosine kinase domains. They bind ligands from the *fgf* family in the presence of heparin and mediate signaling cascades that induce cell growth, differentiation, migration and chemotaxis, angiogenesis, and survival [1,2,4].

Mutations in the FGF receptors have been linked to dysplasias of the skeletal system and the cranium. Many of these pathogenic mutations occur in fibroblast growth factor receptor 3 (FGFR3). Almost all documented FGFR3 mutations are associated with dwarfism syndromes of different severities: achondroplasia (ACH, the most common form of human dwarfism), thanatophoric dysplasia (TD, lethal), and hypochondroplasia (HCH, mild) [3]. It has been demonstrated that FGFR3 dwarfism mutants exhibit higher phosphorylation than wild-type in the absence of ligand [5–8]. Furthermore, the increase in phosphorylation depends on the particular mutation, and higher activation correlates with more severe phenotypes [7]. Thus, a link between a particular dwarfism mutation and enhanced ligand-independent phosphorylation of the corresponding mutant has been established.

A unique pathogenic mutation in FGFR3 was identified in 1995, A391E, leading to disturbances of the growth of the cranium, rather than the long bones. It is the genetic cause for Crouzon syndrome with acanthosis nigricans [9], an autosomal dominant disorder characterized by premature ossification of the skull in the coronal area and skin hyperpigmentation and hyperkeratosis. The A391E mutation has been also identified as a somatic mutation in bladder cancer [10].

Two questions arise: [1] does the A391E mutation enhance ligand-independent activation, similar to the numerous FGFR3 mutations associated with dwarfism phenotypes, and [2] what is the magnitude of this effect, i.e. what is the change in FGFR3 activation propensity due to the mutation? Previous biophysical studies have shown that the A391E mutation stabilizes the isolated FGFR3 TM domain homodimer in lipid bilayers by −1.3 kcal/mol [11,12]. This mechanism could lead to over-stabilization of the unliganded FGFR3 dimers in the plasma membrane, thus increasing ligand-independent activation. If the increase in phosphorylation is due to hydrogen bond-mediated dimer stabilization, then the change in activation propensity will be similar to the value −1.3 kcal/mol measured for dimer stabilization in lipid bilayers.

Thus far, the effect of the mutation has been studied within the context of chimeric receptors, and these studies have produced contradicting results. One study demonstrated that the mutation increases the activation of a chimeric Neu receptor containing the FGFR3 TM domain [13]. In another study, however, the A391E mutation did not affect the downstream signaling of a chimeric PDGF/FGF receptor in the PC12 cell line [14]. To resolve this controversy and to gain insight into the molecular mechanism behind the pathology, here we determine the effect on the A391E mutation on FGFR3 ligand-independent activation within the context of the full-length receptor. We use a method that allows us to determine the change in FGFR3 activation propensity due to the mutation, such that this change can be compared to the dimer stability measurements in lipid bilayers.

* Corresponding author.
E-mail address: khristo1@jhu.edu (K. Hristova).

0005-2736/$ – see front matter © 2011 Elsevier B.V. All rights reserved.
doi:10.1016/j.bbamem.2011.04.007

2. Materials and methods

2.1. Plasmids

The plasmid encoding human wild-type FGFR3 (FGFR3/wt) in the pcDNA 3.1+ vector was a generous gift from Dr. D.J. Donoghue, UCSD. The mutant FGFR3 plasmid (FGFR3/A391E) was produced using a Rapid Change Mutagenesis Kit XL II (Stratagene).

2.2. Cell culture and transfection

Human Embryonic Kidney 293T (HEK 293T) cells were cultured at 37 °C with 5% CO_2 for 24 h. The cells were transfected with plasmids encoding FGFR3/wt and FGFR3/A391E using Fugene 6 (Roche), following the manufacturer's protocol. Varying levels of receptor expression were achieved by varying the amount of plasmid used in transfection. In all cases, cells were starved prior to the experiments, a treatment which induces receptor accumulation in the plasma membrane.

2.3. Immunostaining

Cells were cultured for 24 h after transfection, and then starved for 24 h. After fixing with 4% paraformaldehyde (PFA), the cells were blocked using 3% bovine serum albumin (BSA) for 1 h. Surface localization of FGFR3 in HEK 293T cells was detected with FGFR3 (H-100) antibodies (sc-9007, Santa Cruz Biotechnology), recognizing the extracellular N-terminal domain, followed by FITC-conjugated goat anti rabbit IgG (Invitrogen, CA), without cell permeabilization. Images were acquired under identical conditions using a Nikon confocal microscope.

2.4. Western blots

HEK 293T cells were cultured for 24 h following transfection, starved in serum-free medium for 24 h and then treated with lysis buffer (25 mM Tris-HCl, 0.5% Triton X-100, 20 mM NaCl, 2 mM EDTA, 2 mM $NaVO_4$ and protease inhibitor, Roche Applied Science). The lysates were collected following centrifugation at 15,000 *g* for 15 min at 4 °C and loaded onto 3–8% NuPAGE® Novex® Tris–Acetate mini gels (Invitrogen, CA). The proteins were transferred onto a nitrocellulose membrane, and blocked using 5% milk in TBS. FGFR3 total protein and phosphorylation levels were probed with antibodies against FGFR3 (H-100; sc-9007, Santa Cruz Biotechnology) and phospho-FGFR (Tyr653/654; Cell Signaling Technology), respectively, followed by anti-rabbit HRP conjugated antibodies (W4011, Promega). The proteins were detected using the Amersham ECL detection system (GE Healthcare).

2.5. Titration with fgf1

Cells were starved overnight in serum-free medium, before *fgf1* (Millipore, MA) was added at concentrations ranging from 5 ng/ml to 5000 ng/ml. After incubating for 10 min with *fgf1* the cells were lysed and analyzed by Western blot.

2.6. Quantification of Western blots

The Western blot films were scanned and processed using ImageQuant TL. At least three independent experiments were performed in order to determine averages and standard deviations. For quantification, the amount of protein lysate loaded onto gels was adjusted such that all the band intensities were within the so-called linear range, with intensities proportional to the receptor concentrations [13].

2.7. Flow cytometry measurements

HEK 293T cells were transfected with plasmids encoding the wild-type and mutant FGFR3. Twenty-four hours later, cells were starved in serum-free DMEM for another twenty-four hours. The cells were dislodged from the culture dishes using 5 mM EDTA and washed with ice cold 3% FBS/PBS. FGFR3 expressed on the cell surface was stained with FGFR3 (H-100) antibodies (sc-9007, Santa Cruz Biotechnology). The cells were then incubated in a solution of fluorescein conjugated anti-rabbit IgG (401314, EMD, NJ). Measurements were performed with a FACS Calibur flow cytometer (Beckon Dickinson). HEK 293T cells that were not transfected served as control.

3. Results

3.1. Expression of wild-type and mutant receptors

To study the effect of the A391E mutation on FGFR3 expression, we first performed immunostaining experiments. In these experiments, HEK 293T cells were transfected with plasmids encoding wild-type and mutant FGFR3, starved for 24 h to induce accumulation of receptors on the plasma membrane [15], and immunostained with anti-FGFR3 (H-100, Santa Cruz) antibodies, followed by FITC-conjugated goat anti rabbit IgG (Invitrogen, CA), without cell permeabilization. The results, shown in Fig. 1A, demonstrate that both wild-type and mutant FGFR3 can be detected on the cell surface. While the surface expression varied from cell to cell, there were cells that exhibited very similar staining intensities for the wild-type and the mutant (an example shown in Fig. 1B). A close inspection of Fig. 1A shows, however, that when the cells were transfected with the wild-type plasmid, the number of cells which exhibited membrane fluorescence was greater as compared to the cells transfected with the mutant plasmid. This suggests that the plasma membrane expression of the receptors is decreased due to the mutation.

To gain further insight into the effect of the mutation on plasma membrane expression, we performed flow cytometry experiments after cell starvation as described in Materials and methods. We used an antibody to the extracellular domain of FGFR3 and a fluorescein conjugated anti-rabbit IgG secondary antibody. Fig. 2 compares the results for the wild-type and mutant receptor, when 4 μg DNA was used for transfection. We see that the distribution of cells transfected with either the wild-type or the mutant receptor is shifted to higher fluorescence intensities, as compared to non-transfected cells. In addition, there is a right-shift in the number of cells expressing the wild-type receptor, suggesting that these cells may accumulate a greater number of receptors at the cell surface than cells bearing the A391E mutant receptor. In three independent experiments, cells bearing wild-type FGFR3 exhibited increased fluorescence over A391E-bearing cells (not shown), suggesting that the average concentration of the wild-type receptors at the plasma membrane is greater than that of the A391E receptors.

Next we compared the expression levels of wild-type FGFR3 and the A391E mutant in HEK 293T cells using Western blotting (see Fig. 3). The middle panel in Fig. 3 shows the total receptor levels, while the bottom panel shows an actin loading control. For both wild-type and mutant FGFR3 we observe two bands corresponding to the intermediate, 120 kDa Endo H-sensitive FGFR3 found in the ER/cis-Golgi, and the fully glycosylated mature 130 kDa FGFR3, located predominantly on the plasma membrane [14,16]. Lane 1 corresponds to wild-type FGFR3, while lane 2 corresponds to the mutant receptor, when 1 μg DNA was used for transfection in both cases. From the middle panel in Fig. 3, we see that the intensities of the 120 kDa immature FGFR3 are roughly similar for the wild-type and mutant receptor, suggesting that the synthesis of the 120 kDa

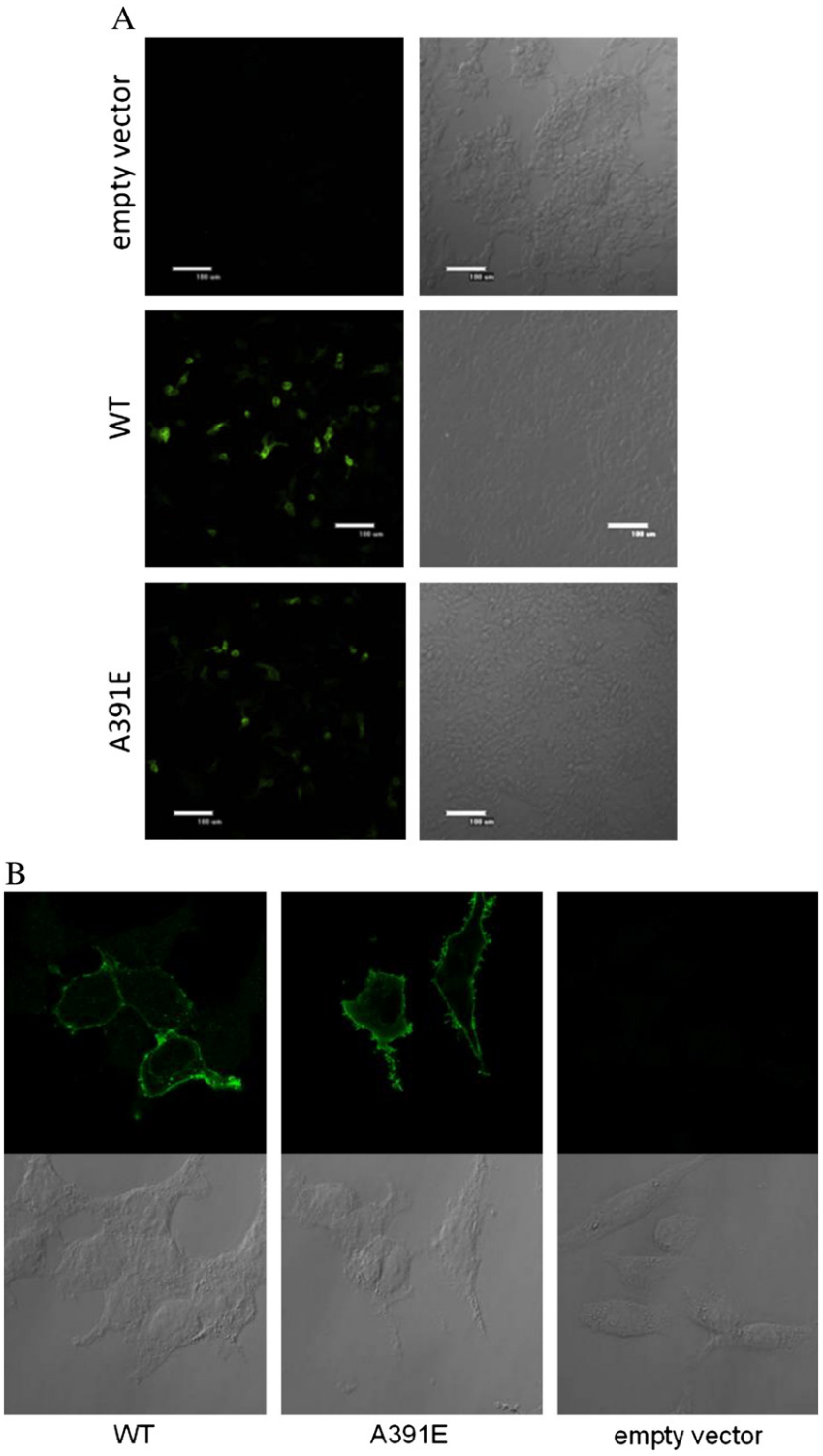

Fig. 1. Immunostaining of HEK 293T cells expressing wild-type and mutant FGFR3 at the plasma membrane. Cells were cultured for 24 h after transfection and serum starved. After fixing with 4% paraformaldehyde (PFA), the cells were blocked using bovine serum albumin (BSA) for 1 h. The cells were incubated with anti-FGFR3 antibodies, followed by FITC-conjugated goat anti rabbit IgG antibodies without cell permeabilization to identify wild-type and mutant receptors localized at the cell surface. (A) 10× objective; (B) 60× objective.

form is not significantly affected by the A391E mutation. The intensity of the mature 130 kDa FGFR3 band, however, is stronger for the wild-type than the mutant receptor. Thus, the expression of the mature FGFR3, located predominantly in the plasma membrane, is lower for the A391E mutant, consistent with the flow cytometry results in Fig. 2.

The immunostaining, flow cytometry, and Western blot results suggest that the expression of the mutant receptor in the plasma membrane is lower than the expression of the wild-type. One possible explanation for this apparent decrease is impaired trafficking of the mutant receptor to the cell surface. There are previous reports about defective trafficking of FGFR3 mutants linked to skeletal dysplasias

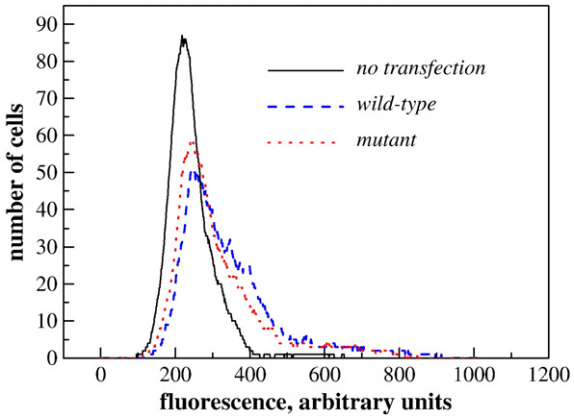

Fig. 2. Flow cytometry data for HEK 293T cells expressing wild-type and mutant FGFR3. Non-transfected cells served as control. FGFR3 expressed on the cell surface was probed using anti-N-FGFR3 antibodies, followed by fluorescein conjugated anti-rabbit IgG antibodies.

[17–19], and thus it appears that the A391E mutation may also cause a similar defect.

3.2. Phosphorylation of wild-type and mutant receptors

Next we investigated whether the A391E mutation affects the phosphorylation of mature FGFR3 in the absence of ligand. The phosphorylation was detected by Western blot using anti-phospho-FGFR antibodies (anti-Y653/654, Cell Signaling Technology) [16]. These antibodies are specific for two phosphorylated tyrosines in the activation loop of FGFR3, Y647 and Y648. The phosphorylation of these two tyrosines is required for the activation of the kinase domain and the phosphorylation of other intracellular tyrosine residues [20].

The top panel in Fig. 3 shows FGFR3 phosphorylation, in the absence of ligand, when 1 μg of DNA is used for transfection. We see that the intensities of the 130 kDa anti-Y653/654 bands of the wild-type and the mutant receptor are similar (top panel), suggesting that the phosphorylation levels are similar, while the total expression is

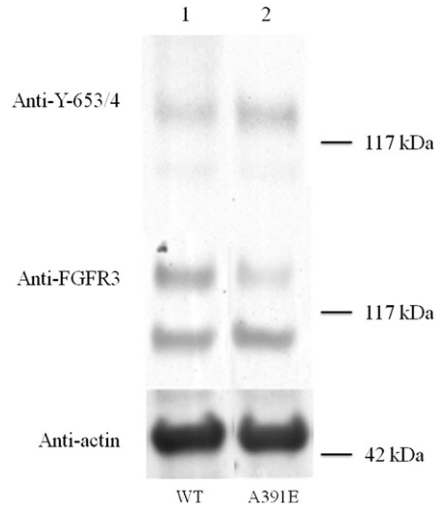

Fig. 3. Expression and phosphorylation of wild-type FGFR3 and the A391E mutant in HEK 293T cells. HEK 293T cells were transfected with 1 μg DNA encoding FGFR3/wt (lane 1) and FGFR3/A391E (lane 2). Cells were lysed after 24-hour culture and 24-hour starvation, and subjected to Western blotting. The blots were probed using anti-FGFR3 antibodies to assess total receptor levels (middle panel) and using anti-Y653/654 antibodies to assess receptor phosphorylation levels (top panel). Actin is shown in the bottom panel. Lanes have been removed for clarity.

lower for the mutant (middle panel). Thus, it appears that the mutation increases receptor phosphorylation in the absence of ligand. Due to the different levels of plasma membrane expression of the wild-type and mutant receptors, however, it is difficult to compare directly the phosphorylation levels for a single set of samples on a Western blot. To be able to carry out such a comparison, we determined the active fractions of the 130 kDa wild-type and mutant receptors as a function of their concentrations, and we calculated their activation propensities, as described below.

We have previously demonstrated that we can determine active RTK fractions if we treat with their ligands and measure RTK phosphorylation over a very wide range of ligand concentrations, including very high ligand concentrations [16]: At high ligand concentration all receptors that are exposed to ligand and capable of binding ligand are driven to their liganded dimeric state [16]. At these levels, phosphorylation is saturated and is not further increased when more ligand is added, providing a measure of the maximum possible phosphorylation. Active receptor fractions in the absence of ligand are then determined as the ratio of measured phosphorylation at zero ligand over the maximum possible phosphorylation [13,16].

We used the ligand *fgf1*, known to bind and activate FGFR3, in these experiments. Fig. 4A shows representative *fgf1* titration experiments for wild-type and mutant FGFR3 at fixed receptor expressions. The top panels show the phosphorylation of the receptors (detected with anti-Y653/654 antibodies), while the bottom panels show the total receptor levels (anti-FGFR3 antibodies). As expected, mature FGFR3, localized primarily on the cell surface, responds to ligand and exhibits an increase in phosphorylation, while the lower molecular weight form of FGFR3, localized to the ER, is not affected. We further see that the phosphorylation increases as more ligand is added until a plateau is reached at high ligand concentration, as anticipated [16]. Special attention was paid to ensure that we saturate receptor phosphorylation and not simply saturate the blotting membrane capacity. As discussed previously [13,16], the band intensities were always within the so-called linear range, where the band intensities are proportional to the receptor concentrations. Here we were interested in the mature fully-glycosylated 130 kDa receptor, and we thus quantified only the 130 kDa band using Image Quant TL. To place the results for the wild-type and the mutant on the same scale, the maximum phosphorylation was assigned a value of 1 at high *fgf1* concentrations. Results are shown in Fig. 4B, and they show a wide plateau region, corresponding to saturating ligand concentrations.

Based on the experiments shown in Fig. 4, the active receptor fraction at a fixed receptor expression, at zero ligand, was measured as follows: We first transfected HEK 293T cells with wild-type or A391E FGFR3, split the cell population after 24 h growth and 24 h of starvation, and then incubated half of the cells with 2500 ng/ml *fgf1* for 10 min. The cells were lysed and receptor phosphorylation was measured using Western blotting. The active fraction was calculated as the ratio: $[P]_0/[P]_{sat}$, where $[P]_0$ is the anti-Y653/654 band intensity in the absence of ligand and $[P]_{sat}$ is the anti-Y653/654 band intensity at saturating ligand concentration (2500 ng/ml *fgf1*).

We measured active fractions at zero ligand, as discussed above, over a wide range of receptor expression, achieved via transfection with different amounts of DNA. To validate the calculations of active fraction for all receptor expression levels, we performed *fgf1* titration experiments such as the one shown in Fig. 4 while varying receptor expression. In each case the phosphorylation was saturated at high ligand concentration. In particular, the phosphorylation in response to 2500 ng/ml *fgf1* was always within the plateau region, no matter how much wild-type or mutant DNA was used for transfection.

The values of $[P]_0/[P]_{sat}$, calculated for various receptor expression levels, are shown with symbols for the wild-type (solid squares) and the A391E mutant (open circles) in Fig. 5. The *x* axis in Fig. 5 is the

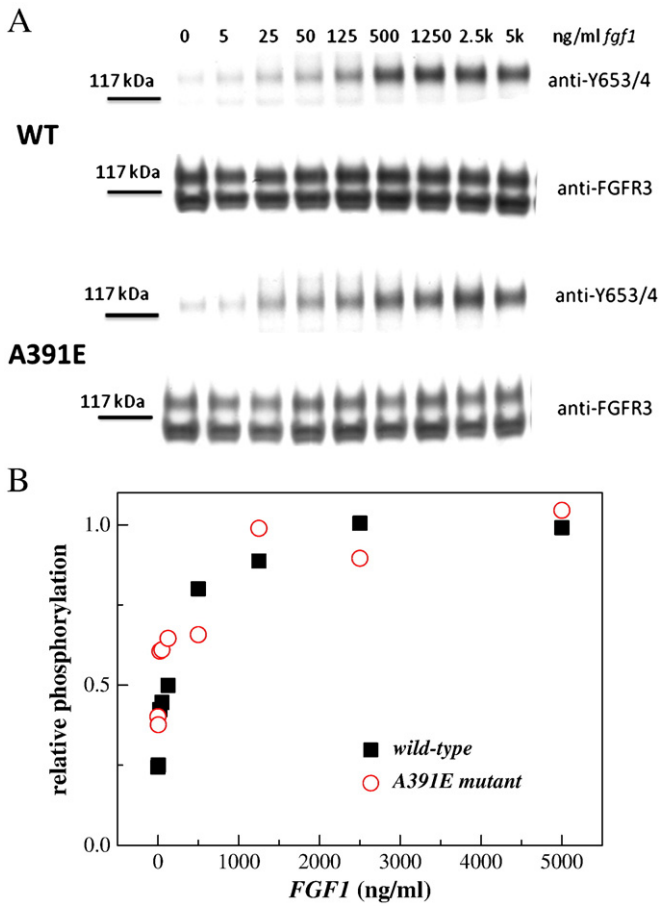

Fig. 4. Effect of *fgf1* concentration on FGFR3 phosphorylation. (A) Representative Western blots, probed using anti-FGFR3 antibodies to assess total receptor levels (bottom) and using anti-Y653/654 antibodies to assess receptor phosphorylation (top). Top: cells transfected with 1 μg of the FGFR3/wt plasmid. Bottom: cells transfected with 2 μg of the FGFR/A391E plasmid. Cells were serum starved for 24 h, then *fgf1* was added for 10 min to the serum-free medium, at concentrations ranging from 5 ng/ml to 5000 ng/ml. The phosphorylation of the mature 130 kDa FGFR3 increased as the ligand concentration increased, and a plateau was reached above the concentration of 1000 ng/ml. (B) Graphical analysis of ligand induced wild-type and A391E receptor phosphorylation. Receptor phosphorylation was proportional to the anti-Y653/654 band intensity and was assigned a value of 1 at saturating *fgf1* concentrations.

estimated concentration of the surface receptors, determined by comparing the expression of the 130 kDa receptors to FGFR3 expression in the stable HEK293-fWT line, estimated to have 8.4×10^5 copies of mature FGFR3 per cell [16], on Western blots. To convert the band intensities to receptor concentrations per unit area of the plasma membrane, we assumed that the surface area of a HEK293T cell is 300 μm^2 (see also [16]).

In Fig. 5 we see that the ligand independent activation of the mature A391E mutant receptor is higher than the activation of the mature wild-type receptor, over a wide range of receptor concentrations. Thus, the A391E mutation increases the propensity of FGFR3 for ligand-independent activation.

3.3. Quantitative assessment of the phosphorylation increase due to the mutation

As discussed previously [13,16,21], the measured active fraction at zero ligand can be fitted to the theoretical prediction of a simple RTK activation model:

$$M + M \overset{K}{\leftrightarrow} D. \tag{1}$$

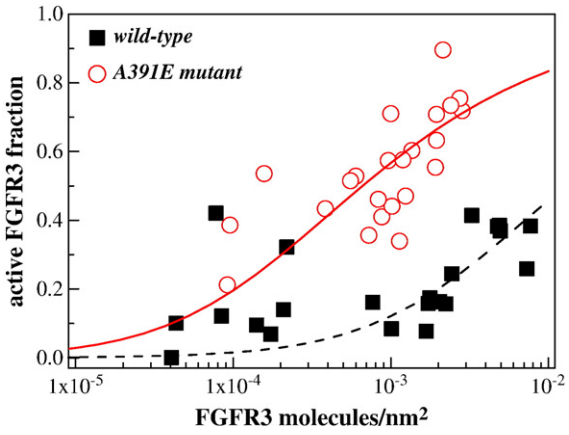

Fig. 5. Active fraction of mature FGFR3 in the absence of ligand, as a function of its expression. Varying levels of receptor expression were achieved by varying the amount of plasmid used for transfection from 0.75 μg to 6 μg of plasmid. Phosphorylated FGFR3 fractions were measured by comparing phosphorylation levels in the absence of ligand and at saturating *fgf1* concentration (2500 ng/ml *fgf1*). The A391E mutant (○) shows a higher phosphorylated fraction than the wild-type (■). The data were fitted to a simple activation model (see scheme (1) and reference [13]), yielding the activation propensities for the wild-type and mutant receptors. The effect of A391E on the activation propensity was calculated as −1.7 kcal/mol.

Scheme (1) assumes that all monomers are inactive and all dimers are active, and describes an apparent equilibrium between the inactive monomers (M) and the active dimers (D) in the absence of ligand. This model has been shown to give an adequate fit of RTK phosphorylation data [13], despite its simplicity. The model does not take explicitly into account all events/interactions that regulate RTK phosphorylation. Rather, all these events contribute to an apparent activation constant K defined as:

$$K = \frac{[D]}{[M]^2}. \tag{2}$$

The active dimer fraction 2[D]/2([D]+[M]) was calculated according to this model as discussed previously [13] and then fitted to the experimentally determined active fractions in Fig. 5. The fits for the wild-type and the mutant are shown in Fig. 5 with the dashed and solid lines, respectively. Each fit yielded the optimal value of the apparent constant K, such that the values of K for the wild-type and mutant receptor can be compared: $K_{WT}=78$ nm^2/receptor for the wild-type and $K_{A391E}=1512$ nm^2/receptor for the mutant. From these values we estimated the change in the activation propensities due to the mutation according to [13]:

$$\Delta\Delta G = -RT\ln\frac{K_{A391E}}{K_{WT}} \tag{3}$$

Using Eq. (3) we calculated that the mutation increases the propensity for activation by $\Delta\Delta G=-1.7$ kcal/mol. As discussed in detail previously [13], this value does not depend on the exact x coordinate in Fig. 5, which is based on some roughly estimated values, such as the area of a HEK 293T cell.

4. Discussion

Mutations responsible for dwarfism syndromes map primarily to fibroblast growth factor receptor 3 (FGFR3). These dwarfism syndromes occur in three different severities: (i) the most common form of human dwarfism (achondroplasia, ACH), (ii) hypochondroplasia (HCH), which is milder than achondroplasia, and (iii) the very severe thanatophoric (lethal) dysplasia (TD) [3]. Examples of FGFR3

mutations that cause these dysplasias are (i) G346E, G375C and G380R for ACH, (ii) V381E for HCH, and (iii) R240C, R248C, S249C, G370C, S371C, and Y373C for TD [3,5,22]. Previous studies have suggested that these mutations increase the ligand-independent activation of FGFR3 [5,6,23–26]. Furthermore, studies of cysteine mutants linked to skeletal dysplasia have demonstrated the formation of disulfide-bonded mutant FGFR3 dimers believed to signal in the absence of ligand [7,26,27].

The A391E mutation in FGFR3 is unique, because it has been linked to craniosynostosis (usually associated with FGFR2 mutations), rather than skeletal dysplasias [3,9,28]. Based on model system findings [11], it has been hypothesized that the mutation leads to dimer over-stabilization and enhanced ligand-independent FGFR3 activation, similarly to mutations linked to skeletal dysplasias. To test this hypothesis, we investigated the effect of the A391E mutation on the activation of full-length FGFR3 in HEK293T cells in the absence of ligand.

One important finding in this work is that the plasma membrane expression of the mutant is lower than the wild-type expression in HEK 293T cells, under identical transfection conditions (see Figs. 2 and 3). It is possible that the difference in plasma membrane expression is specific to the cell type used in this study, or it could be a general effect that occurs in all cell types. Skeletal dysplasia mutations are known to impede the trafficking of other FGFR3 mutant receptors to the plasma membrane, resulting in their intracellular accumulation [5,15,25,29]. Our experiments suggest that a similar trafficking defect may occur due to the A391E mutation, at least in HEK 293T cells. Alternatively, it is possible that the enhanced activation causes enhanced degradation of the activated 130 kDa form of the mutant A391E receptor.

Despite the fact that the plasma membrane expression of the mutant was lower than the wild-type, we were able to compare their phosphorylation (see Fig. 5). Our results demonstrate an increase in FGFR3 phosphorylation due to the A391E mutation in HEK 293T cells. Thus, the effect of the mutation on phosphorylation is similar to the phosphorylation increase observed for the FGFR3 mutants linked to skeletal dysplasias. Results obtained in a recent study of FGFR3 heterodimerization [30] (see data points at zero ligand in Figs. 8A and C [30]), also show an increase in phosphorylation due to the A391E mutation in a related, yet distinctly different cell line, HEK 293.

The major finding of this work is that the A391E mutation increases the activation propensity of full-length FGFR3 by −1.7 kcal/mol. This value is consistent with the observed strength of hydrogen bonds in membranes [31]. It is also similar to the stabilization of the isolated A391E mutant TM domain dimer in lipid bilayers, −1.3 kcal/mol, which is believed to occur due to hydrogen bonding of the side chain of Glu391 with the backbone of the neighboring helix in the homodimer [11,12]. Such an effect represents a change in the physical interactions between the two receptors in the dimer, and is not expected to be cell type-specific (although the composition of the membrane may modulate its strength [32,33]). Thus, the increase in FGFR3 activation due to the A391E mutation that we measure here is consistent with hydrogen-bond mediated stabilization of FGFR3 unliganded dimers in the plasma membrane.

Acknowledgements

Supported by NIH GM068619, NSF MCB 0718841 and research grant 10-POR-007 from Shriners Hospitals for Children. We thank Dr. Lijuan He for many useful discussions.

References

[1] A.O.M. Wilkie, G.M. Morriss-Kay, E.Y. Jones, J.K. Heath, Functions of fibroblast growth factors and their receptors, Curr. Biol. 5 (1995) 500–507.
[2] C.G.M. L'Horte, M.A. Knowles, Cell responses to FGFR3 signaling: growth, differentiation and apoptosis, Experim. Cell Res. 304 (2005) 417–431.
[3] Z. Vajo, C.A. Francomano, D.J. Wilkin, The molecular and genetic basis of fibroblast growth factor receptor 3 disorders: the achondroplasia family of skeletal dysplasias, Muenke craniosynostosis, and Crouzon syndrome with acanthosis nigricans, Endocr. Rev. 21 (2000) 23–39.
[4] V.P. Eswarakumar, I. Lax, J. Schlessinger, Cellular signaling by fibroblast growth factor receptors, Cytokine Growth Factor Rev. 16 (2005) 139–149.
[5] D. Harada, Y. Yamanaka, K. Ueda, H. Tanaka, Y. Seino, FGFR3-related dwarfism and cell signaling, J. Bone Miner. Metab. 27 (2009) 9–15.
[6] Y. Li, K. Mangasarian, A. Mansukhani, C. Basilico, Activation of FGF receptors by mutations in the transmembrane domain, Oncogene 14 (1997) 1397–1406.
[7] M.C. Naski, Q. Wang, J.S. Xu, D.M. Ornitz, Graded activation of fibroblast growth factor receptor 3 by mutations causing achondroplasia and thanatophoric dysplasia, Nat. Genet. 13 (1996) 233–237.
[8] M.K. Webster, D.J. Donoghue, Constitutive activation of fibroblast growth factor receptor 3 by the transmembrane domain point mutation found in achondroplasia, EMBO J. 15 (1996) 520–527.
[9] G.A. Meyers, S.J. Orlow, I.R. Munro, K.A. Przylepa, E.W. Jabs, Fibroblast-growth-factor-receptor-3 (Fgfr3) transmembrane mutation in Crouzon-syndrome with acanthosis nigricans, Nat. Genet. 11 (1995) 462–464.
[10] B. van Rhijin, A. van Tilborg, I. Lurkin, J. Bonaventure, A. de Vries, J.P. Thiery, T.H. van der Kwast, E. Zwarthoff, F. Radvanyi, Novel fibroblast growth factor receptor 3 (FGFR3) mutations in bladder cancer previously identified in non-lethal skeletal disorders, Eur. J. Hum. Genet. 10 (2002) 819–824.
[11] E. Li, M. You, K. Hristova, FGFR3 dimer stabilization due to a single amino acid pathogenic mutation, J. Mol. Biol. 356 (2006) 600–612.
[12] E. Li, K. Hristova, Role of receptor tyrosine kinase transmembrane domains in cell signaling and human pathologies, Biochemistry 45 (2006) 6241–6251.
[13] L. He, K. Hristova, Pathogenic activation of receptor tyrosine kinases in mammalian membranes, J. Mol. Biol. 384 (2008) 1130–1142.
[14] S. Raffioni, Y.Z. Zhu, R.A. Bradshaw, L.M. Thompson, Effect of transmembrane and kinase domain mutations on fibroblast growth factor receptor 3 chimera signaling in PC12 cells. A model for the control of receptor tyrosine kinase activation, J. Biol. Chem. 273 (1998) 35250–35259.
[15] E. Monsonego-Ornan, R. Adar, T. Feferman, O. Segev, A. Yayon, The transmembrane mutation G380R in fibroblast growth factor receptor 3 uncouples ligand-mediated receptor activation from down-regulation, Mol. Cell. Biol. 20 (2000) 516–522.
[16] L. He, W.A. Horton, K. Hristova, The physical basis behind achondroplasia, the most common form of human dwarfism, J. Biol. Chem. 285 (2010) 30103–30114.
[17] P.M.J. Lievens, E. Liboi, The thanatophoric dysplasia type II mutation hampers complete maturation of fibroblast growth factor receptor 3 (FGFR3), which activates signal transducer and activator of transcription 1 (STAT1) from the endoplasmic reticulum, J. Biol. Chem. 278 (2003) 17344–17349.
[18] P.M.J. Lievens, C. Mutinelli, D. Baynes, E. Liboi, The kinase activity of fibroblast growth factor receptor 3 with activation loop mutations affects receptor trafficking and signaling, J. Biol. Chem. 279 (2004) 43254–43260.
[19] J. Bonaventure, L. Gibbs, W.C. Horne, R. Baron, The localization of FGFR3 mutations causing thanatophoric dysplasia type I differentially affects phosphorylation, processing and ubiquitylation of the receptor, FEBS J. 274 (2007) 3078–3093.
[20] M. Mohammadi, I. Dikic, A. Sorokin, W.H. Burgess, M. Jaye, J. Schlessinger, Identification of six novel autophosphorylation sites on fibroblast growth factor receptor 1 and elucidation of their importance in receptor activation and signal transduction, Mol. Cell. Biol. 16 (1996) 977–989.
[21] J.L. Macdonald, L.J. Pike, Heterogeneity in EGF-binding affinities arises from negative cooperativity in an aggregating system, Proc. Natl. Acad. Sci. U. S. A. 105 (2008) 112–117.
[22] W.A. Horton, J.G. Hall, J.T. Hecht, Achondroplasia, Lancet 370 (2007) 162–172.
[23] R. Shiang, L.M. Thompson, Y.-Z. Zhu, D.M. Church, T.J. Fielder, M. Bocian, S.T. Winokur, J.J. Wasmuth, Mutations in the transmembrane domain of FGFR3 cause the most common genetic form of dwarfism, achondroplasia, Cell 78 (1994) 335–342.
[24] M.K. Webster, D.J. Donoghue, FGFR activation in skeletal disorders: too much of a good thing, Trends Genet. 13 (1997) 178–182.
[25] J.Y. Cho, C.S. Guo, M. Torello, G.P. Lunstrum, T. Iwata, C.X. Deng, W.A. Horton, Defective lysosomal targeting of activated fibroblast growth factor receptor 3 in achondroplasia, Proc. Natl. Acad. Sci. U. S. A. 101 (2004) 609–614.
[26] M. You, J. Spangler, E. Li, X. Han, P. Ghosh, K. Hristova, Effect of pathogenic cysteine mutations on FGFR3 transmembrane domain dimerization in detergents and lipid bilayers, Biochemistry 46 (2007) 11039–11046.
[27] R. Adar, E. Monsonego-Ornan, P. David, A. Yayon, Differential activation of cysteine-substitution mutants of fibroblast growth factor receptor 3 is determined by cysteine localization, J. Bone Miner. Res. 17 (2002) 860–868.
[28] I. Mcintosh, G.A. Bellus, E.W. Jabs, The pleiotropic effects of fibroblast growth factor receptors in mammalian development, Cell Struct. Funct. 25 (2000) 85–96.
[29] E. Monsonego-Ornan, R. Adar, E. Rom, A. Yayon, FGF receptors ubiquitylation: dependence on tyrosine kinase activity and role in downregulation, FEBS Lett. 528 (2002) 83–89.
[30] L. He, W.C. Wimley, K. Hristova, FGFR3 heterodimerization in achondroplasia, the most common form of human dwarfism. J. Biol. Chem. 286 (2011), 13272–1328.
[31] N.H. Joh, A. Min, S. Faham, J.P. Whitelegge, D. Yang, V.L. Woods, J.U. Bowie, Modest stabilization by most hydrogen-bonded side-chain interactions in membrane proteins, Nature 453 (2008) 1266-1U73.
[32] S. Schick, L.R. Chen, E. Li, J. Lin, I. Koper, K. Hristova, Assembly of the M2 tetramer is strongly modulated by lipid chain length, Biophys. J. 99 (2010) 1810–1817.
[33] V. Anbazhagan, D. Schneider, The membrane environment modulates self-association of the human GpA TM domain—implications for membrane protein folding and transmembrane signaling, Biochim. Biophys. Acta Biomembr. 1798 (2010) 1899–1907.